

# High Capacity Li Ion Battery Anodes Using Ge Nanowires

Candace K. Chan,<sup>†</sup> Xiao Feng Zhang,<sup>‡</sup> and Yi Cui<sup>\*‡</sup>

*Department of Chemistry, Stanford University, Stanford, California 94305, Electron Microscope Division, Hitachi High Technologies, Pleasanton, California 94588, and Department of Materials Science & Engineering, Stanford University, Stanford, California 94305*

Received October 21, 2007

## ABSTRACT

Ge nanowire electrodes fabricated by using vapor–liquid–solid growth on metallic current collector substrates were found to have good performance during cycling with Li. An initial discharge capacity of 1141 mA·h/g was found to be stable over 20 cycles at the C/20 rate. High power rates were also observed up to 2C with Coulombic efficiency > 99%. Structural characterization revealed that the Ge nanowires remain intact and connected to the current collector after cycling. Nanowires connected directly to the current collector have facile strain relaxation and material durability, short Li diffusion distances, and good electronic conduction. Thus, Ge nanowire anodes are promising candidates for the development of high-energy-density lithium batteries.

There has been much research interest in the development of higher-specific-energy lithium batteries,<sup>1</sup> particularly in higher-capacity alternatives for the Li–graphite anode, which has a maximum theoretical specific capacity of 372 mA·h/g. Important requirements for useful alternative materials include a large discharge capacity at potentials not far from that of elemental Li, the ability to sustain high currents, and good reversibility for an attractive rechargeable cycle life. A number of metal and metal–metalloid materials such as Si, Sn, Al, and Bi have been known to alloy with large amounts of Li but have had limited application due to large volume changes during lithium insertion and deinsertion.<sup>2</sup> Si, for example, has the largest theoretical capacity known of 4200 mA·h/g but also undergoes a 400% change in volume, leading to decrepitation and loss of electrical contact in bulk electrodes.<sup>3</sup> To facilitate strain relaxation and improve conductivity, Si nanowires (NWs) grown directly on current collector substrates using the vapor–liquid–solid (VLS) growth method were found to display much higher capacities than other structured forms of Si.<sup>4</sup> The improved performance of the SiNWs is attributed to good electronic conduction along the length of each NW, short Li insertion distances, high interfacial contact area with electrolyte, good electrical contact between each NW and the current collector, and improved material durability due to nanostructuring. NW electrodes of other Li battery materials have also shown improved electrochemical behavior.<sup>5–9</sup>

The analogous Li<sub>x</sub>Ge system has received little attention. The fully lithiated Li<sub>4.4</sub>Ge has a high theoretical capacity of 1600 mA·h/g and undergoes a volume change of 370%. The room-temperature diffusivity of Li in Ge is 400 times higher than that in Si,<sup>10</sup> indicating that Ge may be an attractive electrode material for high-power-rate anodes. Nanocomposites of Ge with carbon<sup>11,12</sup> and tin<sup>13</sup> have shown promising capacity and cyclability. Here, we report the synthesis of GeNWs directly onto metal current collector substrates for use as Li battery anodes. Compared to previous studies,<sup>11–13</sup> this design is advantageous because of the ease of fabrication of our electrode. Fabrication of the traditional battery electrode, shown schematically in Figure 1a, often involves mixing of the active material with conducting carbon and a nonconducting polymeric binder (such as polyvinylidene fluoride) and then casting it onto the current collector as a slurry followed by annealing for several hours. In contrast, our NW electrode (Figure 1b) is fabricated in one step during the NW synthesis without any post-growth processing needed. By using the growth substrate as the current collector, our fabrication is faster and easier. Additionally, our NW electrode design has several advantages. First, there is good electrical contact between the current collector and every NW so that more active material can contribute to the capacity. For materials that undergo large volume changes during reactions with Li, often times, active material loses electronic contact due to pulverization and insufficient binding power of the polymer. With each NW contacting the current collector, this problem is avoided. Second, NWs have good materials properties that make them attractive as electrode materials. The small diameter and 1D conductivity

\* To whom correspondence should be addressed. E-mail: yicui@stanford.edu.

<sup>†</sup> Department of Chemistry, Stanford University.

<sup>‡</sup> Hitachi High Technologies.

<sup>‡</sup> Department of Materials Science & Engineering, Stanford University.

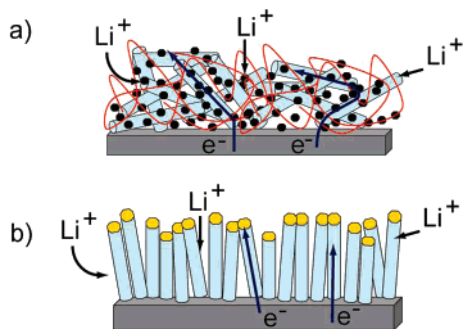


**Figure 1.** (a) A traditional battery electrode consisting of a composite of active material (blue rods), amorphous carbon to enhance conductivity (black circles), and a polymeric binder (red line). Disadvantages of this electrode design include poor electron transport from the current collector due to disconnected material, loss of active material due to insufficient binding power of the polymer, and lower specific capacity due to extra weight of the additives. (b) NW electrode design consisting of NWs (blue rods) grown directly on the current collector. The gold circles on the tips of the NWs are the catalyst used in the synthesis. Advantages of this electrode design include good electrical contact between the current collector and all NWs, good charge transport along the length of the NW, facile fabrication, and no additives needed.

can allow for facile volume changes without pulverization and efficient charge transport, both for Li ions from the electrolyte and electrons from the current collector. Finally, no binders or conducting carbon are needed, which add extra weight and lower the overall specific capacity of the battery.

GeNWs were synthesized using VLS<sup>14–18</sup> growth using chemical vapor deposition (CVD)<sup>19</sup> from GeH<sub>4</sub> decomposition onto metallic substrates (stainless steel foil) covered with Au catalyst (Supporting Information). Compared to template-mediated<sup>5</sup> growth of NWs, for example, into anodized aluminum oxide pores on a metallic substrate, using VLS growth has the advantage of producing single-crystalline materials and requires fewer fabrication steps. GeNW growth on stainless steel (SS) using the typical conditions for growing NWs on a Si substrate was found to lead to poor adhesion between the NWs and the SS. Thus, a high-temperature (520 °C) annealing step for 5 min under GeH<sub>4</sub> flow preceding the lower-temperature (320 °C) GeNW growth was found to help adhesion of the GeNWs onto the SS by promoting good contact due to the interfacial Fe–Ge alloy formation. In fact, ~85% of the sample remained adhered to the SS even after ultrasonication of the sample for ~1 min.

The electrochemical properties were evaluated under an Ar atmosphere by galvanostatic cycling in a two-electrode configuration, with the GeNWs on the SS substrate as the working electrode and Li foil as the counter electrode. The charge capacity referred to here is the total charge inserted per unit mass of the GeNWs during Li insertion, whereas the discharge capacity is the total charge removed during Li extraction.

The electrochemical cycling of the GeNWs was found to be stable for 20 cycles at the C/20 rate, or 20 h per half-cycle (Figure 2a). The first charge capacity was 2967 mA·h/g, and the first discharge capacity was 1141 mA·h/g, indicating a Coulombic efficiency of 39%. Because the

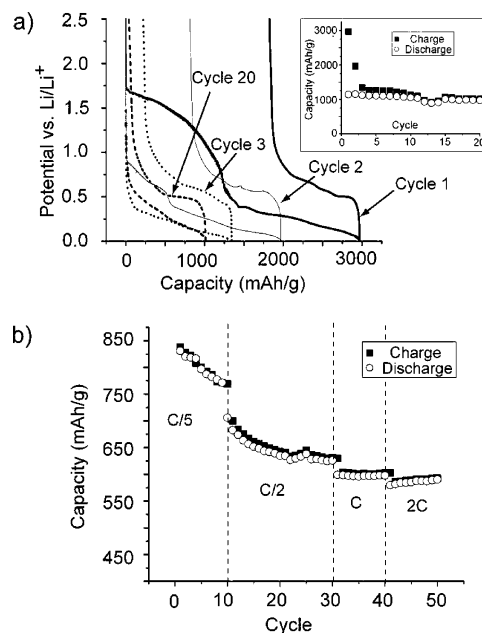


**Figure 2.** (a) Constant current voltage profile at the C/20 rate for GeNWs with the cycle life in the inset. (b) Cycling at different discharge rates with a charge rate of C/20. These cycles were performed after initial C/20 cycles.

charge capacity is greater than the theoretical capacity (1600 mA·h/g), the irreversible capacity loss is likely due to reactions at the surface of the NWs. One possibility is the formation of a surface–electrolyte interphase (SEI) film due to electrolyte decomposition. This has been well studied in carbonaceous electrodes<sup>20</sup> and has been observed in Ge<sup>10</sup> and Si electrodes.<sup>21</sup>

The second possibility is the decomposition of the native oxide that forms on the GeNWs. Metal oxide decomposition upon reaction with Li, that is,  $MO + 2Li \rightarrow M + Li_2O$ , has been observed for many systems.<sup>5,22,23</sup> The irreversible decomposition of GeO<sub>2</sub> to Ge and Li<sub>2</sub>O and the subsequent reversible reaction of the Ge with Li results in a theoretical capacity of about 1380 mA·h/g. The large capacities between ~400 mV and 1.7 V suggest that one or both of these processes may be occurring. The low Coulombic efficiency is limited to the first two cycles, suggesting that any surface reactions occur only during the initial cycling. More studies will be done to determine the exact processes and the origin of the large initial irreversible capacity loss. The Coulombic efficiency for the third 20th cycle is 84–96%, showing excellent reversible cycling after the surface reactions are completed. The discharge capacity remains stable at ~1000 mA·h/g over 20 cycles (Figure 2a, inset), indicating that the GeNWs remain contacted to the current collector and do not undergo pulverization.

High rate capabilities were also observed in the NWs (Figure 2b). Discharging at C/5, C/2, C, and 2C (the charge was fixed at C/20) revealed good cyclability. The Coulombic efficiency of 99% was also quite high, indicating excellent reversibility. The capacity was very stable at the high C and 2C rates, indicating good Li diffusivity in the GeNWs. Although the capacity dropped at the 2C rate to ~600 mA·h/g, it was still much higher than the graphite capacity of 372 mA·h/g.

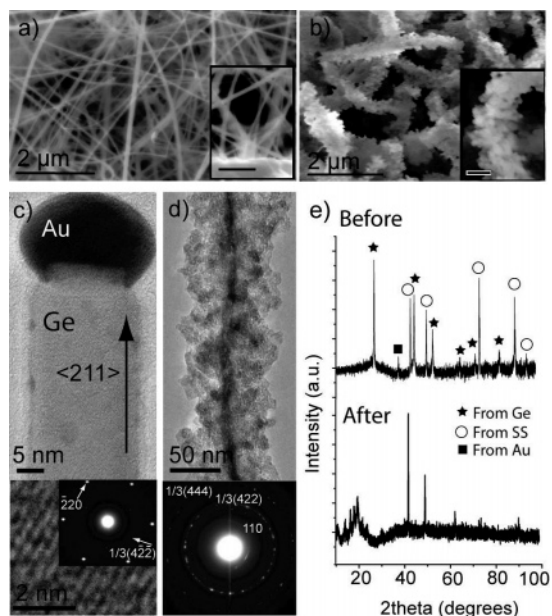


**Figure 3.** (a) SEM image of as-grown GeNWs on SS. Inset, cross-sectional view (scale bar, 500 nm). (b) SEM image of GeNWs on SS after Li cycling. The magnification is the same as that in Figure 3a. Inset, zoomed-in view of a textured NW (scale bar, 250 nm). (c) TEM image and SAED of as-grown GeNW on the [111] zone axis. HRTEM shows the  $1/3(422)$  lattice fringes. (d) TEM image and SAED of GeNW after Li cycling. The NW becomes mostly amorphous with some small Ge crystalline grains as indexed from the SAED. (e) XRD of GeNWs before and after Li cycling.

The structural changes of the GeNWs after lithiation were studied using scanning electron microscopy (SEM), transmission electron microscopy (TEM), and X-ray diffraction (XRD). The as-grown NWs were 50–100 nm in diameter and 20–50  $\mu\text{m}$  long. SEM imaging revealed that the GeNWs grew vertically oriented off of the substrate (Figure 3a). Cross-section SEM showed each NW contacted to the substrate (Figure 3a, inset). The as-grown NWs were single-crystalline, as confirmed by TEM (Figure 3c). Peaks corresponding to Ge and the Au catalyst were observed using XRD (Figure 3e).

Contrary to previous work done on Ge films,<sup>10</sup> where numerous Li–Ge crystalline phases were observed during lithiation, the GeNWs become predominately amorphous during electrochemical cycling, similar to what has been observed in SiNWs.<sup>4</sup> This was observed by the disappearance of the Ge peaks in the XRD (Figure 3e). The low-angle peaks at  $\sim 20^\circ$  were from lithiation of the Au catalyst to form  $\text{Li}_{15}\text{Au}_4$ . Capacity contribution from Au was determined to be negligible in control experiments.<sup>4</sup> SEM (Figure 3b) and TEM (Figure 3d) studies found that the NWs became roughly textured but remained adhered to the substrate. The diameter of the NWs also appears to have increased after lithiation, as expected from the predicted volume change. In addition to the dominant amorphous phase, a polycrystalline diffraction pattern was observed in the TEM, with rings corresponding to Ge. The Ge grains may be either pristine Ge that was never lithiated (and can be attributed to the darker contrast region observed in the core of the NW in Figure 3d) or Ge that recrystallized under delithiation, which has been observed in thin films.<sup>10</sup> It is important to note that the

GeNWs do not pulverize after cycling. This is in contrast to previous studies on Ge thin films,<sup>10</sup> nanocrystals,<sup>11</sup> and NW composites,<sup>13</sup> where fracture and decrepitation were observed.

In conclusion, we have shown that GeNW anodes have a high specific capacity and excellent cycling performance. Our GeNW anode design is easy to fabricate and has good electronic contact between each NW and the current collector. Thus, GeNWs may be a promising, higher-capacity alternative for the existing graphite anode in Li ion batteries.

**Acknowledgment.** We thank Professors Brongersma and Clemens for technical help. Y.C. acknowledges support from the Stanford New Faculty Startup Fund and Global Climate and Energy Project. C.K.C. acknowledges support from a National Science Foundation Graduate Fellowship and Stanford Graduate Fellowship.

**Supporting Information Available:** Materials and methods. This material is available free of charge via the Internet at <http://pubs.acs.org>.

## References

- (1) Nazri, G.-A.; Pistoia, G. *Lithium Batteries: Science and Technology*; Kluwer Academic/Plenum: Boston, MA, 2004.
- (2) Huggins, R. A. *J. Power Sources* **1999**, *81–82*, 13–19.
- (3) Kasavajjula, U.; Wang, C.; Appleby, A. J. *J. Power Sources* **2007**, *163*, 1003–1039.
- (4) Chan, C. K.; Peng, H.; Liu, G.; McIlwrath, K.; Zhang, X. F.; Cui, Y. *Nat. Nanotechnol.* **2007** (advanced online publication), DOI: 10.1038/nnano.2007.411.
- (5) Li, N.; Martin, C. R. *J. Electrochem. Soc.* **2001**, *148*, A164–A170.
- (6) Armstrong, G.; Armstrong, A. R.; Bruce, P. G.; Reale, P.; Scrosati, B. *Adv. Mater.* **2006**, *18*, 2597–2600.
- (7) Park, M.-S.; Wang, G.-X.; Kang, Y.-M.; Wexler, D.; Dou, S.-X.; Liu, H.-K. *Angew. Chem., Int. Ed.* **2007**, *46*, 750–753.
- (8) Nam, K. T.; Kim, D.-W.; Yoo, P. J.; Chiang, C.-Y.; Meethong, N.; Hammond, P. T.; Chiang, Y.-M.; Belcher, A. M. *Science* **2006**, *312*, 885–888.
- (9) Kim, D.-W.; Hwang, I.-S.; Kwon, S. J.; Kang, H.-Y.; Park, K.-S.; Choi, Y.-J.; Choi, K.-J.; Park, J.-G. *Nano Lett.* **2007**, *7*, 3041–3045.
- (10) Graetz, J.; Ahn, C. C.; Yazami, R.; Fultz, B. *J. Electrochem. Soc.* **2004**, *151*, A698–A702.
- (11) Lee, H.; Kim, H.; Doo, S.-G.; Cho, J. *J. Electrochem. Soc.* **2007**, *154*, A343–A346.
- (12) Gao, B.; Sinha, S.; Fleming, L.; Zhou, O. *Adv. Mater.* **2001**, *13*, 816–819.
- (13) Lee, H.; Cho, J. *Nano Lett.* **2007**, *7*, 2638–2641.
- (14) Morales, A. M.; Lieber, C. M. *Science* **1998**, *279*, 208–211.
- (15) Huang, M. H.; Wu, Y.; Feick, H.; Tran, N.; Weber, E.; Yang, P. *Adv. Mater.* **2001**, *13*, 113–116.
- (16) Dick, K. A.; Deppert, K.; Karlsson, L. S.; Wallenberg, L. R.; Samuelson, L.; Seifert, W. *Adv. Funct. Mater.* **2005**, *15*, 1603–1610.
- (17) Wang, Y.; Schmidt, V.; Senz, S.; Gosele, U. *Nat. Nanotechnol.* **2006**, *1*, 189.
- (18) Pan, Z. W.; Dai, Z. R.; Wang, Z. L. *Science* **2001**, *291*, 1947–1949.
- (19) Wang, D.; Dai, H. *Angew. Chem., Int. Ed.* **2002**, *41*, 4783–4786.
- (20) Aurbach, D. The Role of Surface Films on Electrodes in Li-Ion Batteries. In *Advances in Lithium-Ion Batteries*; van Schalkwijk, W. A., Scrosati, B., Eds.; Kluwer Academic/Plenum Publishers: New York, 2002; pp 7–77.
- (21) Lee, Y. M.; Lee, J. Y.; Shim, H.-T.; Lee, J. K.; Park, J.-K. *J. Electrochem. Soc.* **2007**, *154*, A515–A519.
- (22) Poizot, P.; Laruelle, S.; Grugeon, S.; Dupont, L.; Tarascon, J.-M. *Nature* **2000**, *407*, 499.
- (23) Pena, J. S.; Sandu, I.; Joubert, O.; Pascual, F. S.; Arean, C. O.; Brousse, T. *Electrochem. Solid-State Lett.* **2004**, *7*, A278–A281.

NL0727157